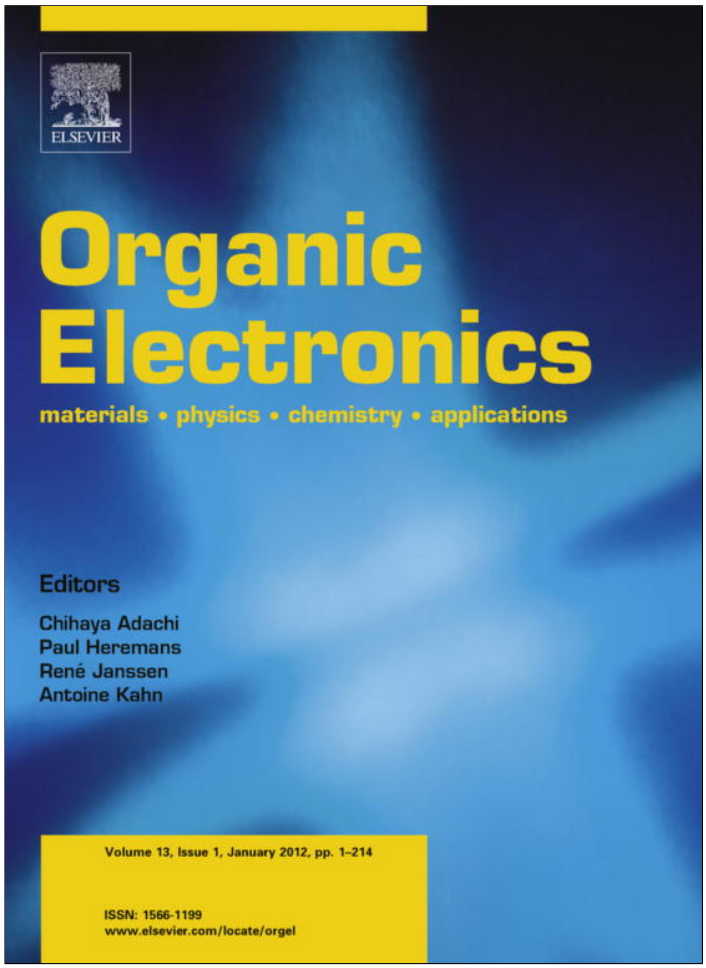

(This is a sample cover image for this issue. The actual cover is not yet available at this time.)

Organic Electronics 13 (2012) 840–849

Contents lists available at SciVerse ScienceDirect

Organic Electronics

journal homepage: www.elsevier.com/locate/orgel

Preparation and characterization of near-infrared and multi-colored electrochromic aramids based on aniline-derivatives

Li-Ting Huang, Hung-Ju Yen, Jia-Hao Wu, Guey-Sheng Liou *

Functional Polymeric Materials Laboratory, Institute of Polymer Science and Engineering, National Taiwan University, 1 Roosevelt Road, 4th Sec., Taipei 10617, Taiwan

ARTICLE INFO

Article history:
Received 14 December 2011
Received in revised form 23 January 2012
Accepted 29 January 2012
Available online 18 February 2012

Keywords:
Polyamides
Electrochemistry
High performance polymer
Polycondensation
Electrochromic materials

ABSTRACT

Two series of novel polyamides **I-II** with diphenylamine (DPA) and triphenylamine (TPA)-derivatives were prepared *via* the low temperature polycondensation from two kinds of synthesized diamines and diacid chlorides, respectively. The aromatic polyamides had useful level of thermal stability associated with relatively high glass-transition temperatures (T_g) (252–275 °C), 10% weight-loss temperatures (T_d^{10}) nearly in excess of 430 °C, and char yield at 800 °C in nitrogen higher than 55%. Due to the additional 4-methoxy-phenyl ring which can provide additional route to stabilize the cation radical formed during oxidation, the TPA-based polyamides **III** revealed more stable electrochemical oxidation behavior and better electrochromic reversibility than DPA-based polyamides. In addition, the prepared electrochromic films had high coloration efficiency, low switching time, and good redox stability.

1. Introduction

Polyaniline (PANI) is an important organic conducting polymer for commercial applications, such as electrochromic display [1], chemical and electromagnetic actuator [2], rechargeable batteries [3], and anti-corrosion coatings [4]. However, PANI synthesized by chemical and electrochemical methods usually exhibited an ill-defined molecular structure and had limited solubility in common of organic solvents. Therefore, oligoanilines can be considered as good model compounds of PANI, which exhibited well-defined structure, easily processible, and even designed the electroactive polymers containing aniline oligomer for applications. Recent studies in preparing polyamides with aniline oligomer has focused on the synthesis of macromonomer [5] to proceed oxidative coupling polymerization or using oligoaniline bearing an orthogonal *tert*-butoxycarbonyl (BOC) group [6] as a monomer to react with acyl chlorides *via* the polycondensation. These resulting polymers have been successfully synthesized and investigated on their thermal properties, electrochemical properties, and multicolored nature, but the long-term stability of aniline-derivative polyamides were rarely mentioned. In addition, the rigidity of the backbone and strong hydrogen bonding of conjugated polyamides result in high glass-transition temperatures and limited solubility in most organic solvents. To overcome such a dilemma, introduction of bulky and packing-disruptive groups into the polymer backbone is a feasible approaching [7]. Since 2005, our groups have initiated several high-performance polymers (*e.g.*, aromatic polyamides and polyimides) utilizing the triphenylamine (TPA) units as a hole-transporting and electrochromic functional moiety [8]. Because of the introduction of packing-disruptive TPA units into the polymer backbone, most of the polymers exhibited good solubility in polar organic solvents, thus transparent and flexible polymer thin films could be prepared easily by solution casting and spin-coating techniques.

In this article, we therefore synthesized new series of polyamides containing TPA and diphenylamine (DPA) moieties *via* low-temperature polycondensation from 4,4′-bis[(4-aminophenyl)amino]-4″-methoxytriphenylamine (**2**), and another series of DPA-derivatives

* Corresponding author.
E-mail address: gsliou@ntu.edu.tw (G.-S. Liou).

1566-1199/$ - see front matter © 2012 Elsevier B.V. All rights reserved.
doi:10.1016/j.orgel.2012.01.025

polyamides from 4,4′-bis[(4-aminophenyl)amino]-diphenyl amine (**1**). The general properties such as solubility, viscosity, and thermal properties are described. For a comparative study, electrochemical and electrochromic properties of the present polyamides were also compared with that of structurally related one based on 4,4′-bis[4-aminophenyl(4-methoxyphenyl)amino]-4″-methoxytriphenylamine (**3**) that has been reported previously [8l].

2. Experimental section

2.1. Materials

4,4′-Bis[(4-aminophenyl)amino]-diphenylamine (**1**) and 4,4′-bis[(4-aminophenyl)amino]-4″-methoxytriphenylamine (**2**) (mp = 77–79 °C), were prepared according to the previously reported procedure [9]. Commercially available diacid chlorides such as isophthaloyl dichloride (**3a**), and terephthaloyl dichloride (**3b**) were purchased from Tokyo Chemical Industry (TCI) Co. and used as received. Commercially obtained anhydrous calcium chloride ($CaCl_2$) was dried under vacuum at 180 °C for 8 h. Tetrabutylammonium perchlorate (TBAP) (Acros) was recrystallized twice by ethyl acetate under nitrogen atmosphere and then dried *in vacuo* prior to use. All other reagents were used as received from commercial sources.

2.2. Preparation of polyamides via low-temperature solution method

The synthesis of polyamide **IIb′** was used as an example to illustrate the general synthetic route used to produce the series of polyamides. The solution of 0.05 g of $CaCl_2$, and 0.24 g (0.50 mmol) of diamine **2** in 1.0 mL of NMP was mechanically stirred at room temperature. Until the salts and diamine monomer dissolved completely, liquid nitrogen with ice-bath was used to freeze the solution. And then, 0.10 g (0.50 mmol) of diacid chloride TPC (**3b**) was added in one portion (25 wt.% solid content). When the mixture started stirring, 0.10 mL (1.50 mmol) of propylene oxide or 0.05 g of CaO was added to the solution. The mixture was mechanically stirred and kept at low temperature (*ca.* −10 °C) for about 3 h. The resulting polymer solution was poured into 100 mL of water giving a dark green precipitate, which was washed thoroughly with hot water and methanol and collected by filtration. The other polyamides were prepared by an analogous procedure. The obtained polyamide **IIb′** only can dissolve in H_2SO_4, and the inherent viscosity was 0.93 dL/g (measured at a concentration of 0.5 g/dL in H_2SO_4 at 30 °C) revealing that the polymer with high molecular weight was obtained. However, because of the poor solubility of polyamide **IIb′** that could not be practical for characterization, therefore we synthesized the polyamide **IIb**, which without adding salts in the polymerization procedure to control the molecular weight for further investigation of electrochemical properties. The inherent viscosities, weight-average molecular weights (M_w), and polydispersity index (PDI) of the obtained polyamide **IIb** was 0.61 dL/g (measured at a concentration of 0.5 g/dL in DMAc at 30 °C), 83,000 daltons, and 1.54, respectively. The FT-IR spectrum of **IIb** (film) exhibited characteristic amide absorption bands at around 3330 (N-H stretching), and 1651 cm^{-1} (amide C=O). 1H NMR (500 MHz, DMSO-d_6, δ, ppm):10.20 (s, 2H, -NH-CO-), 8.06 (s, 4H, H_i), 7.97 (s, 2H, H_f), 7.61 (d, 4H, H_h), 7.03–6.99 (m, 8H, $H_e + H_g$), 6.94 (d, 2H, H_c), 6.87 (d, 6H, $H_b + H_d$), 3.73 (s, 3H, H_a). Anal. Calcd (%) for $C_{39}H_{31}N_5O_3$ (617.70): C, 75.83%; H, 5.06%; N, 11.34%. Found: C, 73.78%; H, 5.18%; N, 10.83%. The IR and ^{1}H NMR spectra of **IIb** are shown in the Supporting information (see Figs. S1 and S2).

2.3. Preparation of the polyamide films

A solution of the polymer was made by dissolving about 0.2 g of the polyamide sample in 6 mL of NMP. The homogeneous solution was poured into a 5 cm glass Petri dish, which was heated in oven at 80 °C for 5 h to remove most of the solvent; then the semi-dried film was further dried *in vacuo* at 180 °C for 10 h. The obtained films were about 70–80 μm thick and were used for solubility tests and thermal analyses.

2.4. Fabrication of the electrochromic device

Electrochromic polymer films were prepared by dropping solution of the polyamide **IIb** (1 mg mL^{-1} in DMAc) onto an ITO-coated glass substrate (20 × 30 × 0.7 mm, 50–100 Ω/square). The polymers were drop-coated onto an active area (about 20 × 20 mm^2) then dried in vacuum. A gel electrolyte based on PMMA (Mw: 350,000) and $LiClO_4$ was plasticized with propylene carbonate to form a highly transparent and conductive gel. PMMA (3 g) was dissolved in dry acetonitrile (15 g), and $LiClO_4$ (0.3 g) was added to the polymer solution as supporting electrolyte. Then, propylene carbonate (5 g) was added as plasticizer. The gel electrolyte was spread on the polymer-coated side of the electrode, and the electrodes were sandwiched. Finally, an epoxy resin was used to seal the device.

2.5. Measurements

Fourier transform infrared (FT-IR) spectra were recorded on a PerkinElmer Spectrum 100 Model FT-IR spectrometer. Elemental analyses were run in a HeraeusVarioEL-III CHNS elemental analyzer. ^{1}H NMR spectra were measured on a Bruker AVANCE-500 FT-NMR using tetramethylsilane as the internal standard, and peak multiplicity was reported as follows: s, singlet; d, doublet. The inherent viscosities were determined at 0.5 g/dL concentration using Tamson TV-2000 viscometer at 30 °C. Gel permeation chromatographic (GPC) analysis was carried out on a Waters chromatography unit interfaced with a Waters 2410 refractive index detector. Two Waters 5 μm Styragel HR-2 and HR-4 columns (7.8 mm I.D. × 300 mm) were connected in series with NMP as the eluent at a flow rate of 0.5 mL/min at 40 °C and were calibrated with polystyrene standards. Thermogravimetric analysis (TGA) was conducted with a PerkinElmer Pyris 1 TGA. Experiments were carried out on approximately 6–8 mg film samples heated in flowing nitrogen or air (flow rate = 20 cm^3/min) at a heating rate of 20 °C/min. DSC analyses were performed on a

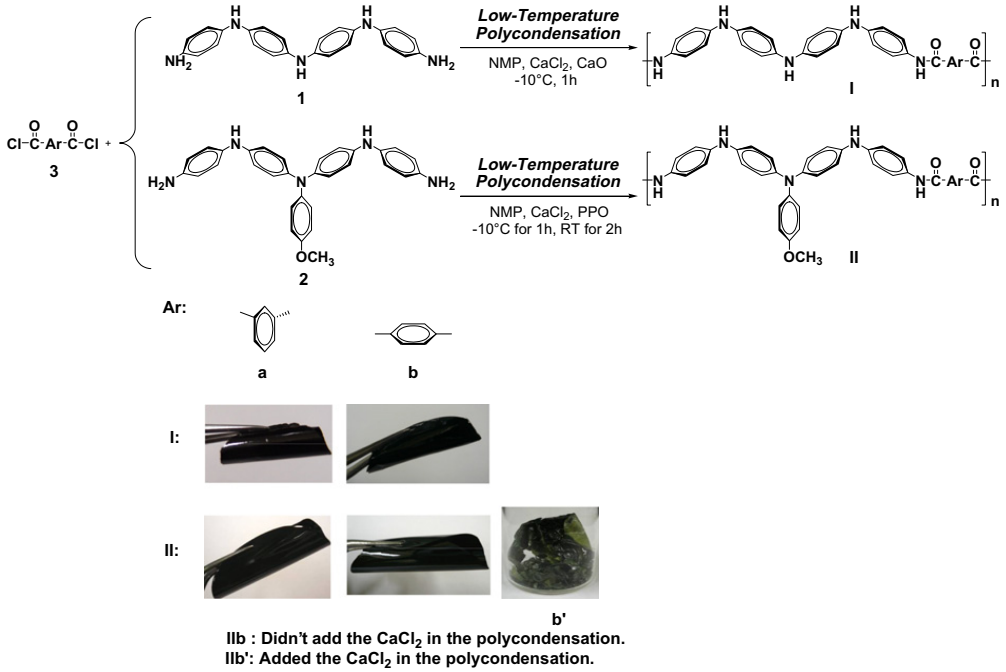

Scheme 1. Synthesis of aromatic polyamides **Ia-Ib** and **IIa-IIb**. Photographs show appearance of these polymer flexible films.

PerkinElmer Pyris 1 DSC at a scan rate of 20 °C/min in flowing nitrogen (20 cm^3/min). Electrochemistry was performed with a CH Instruments 611B electrochemical analyzer. Voltammograms are presented with the positive potential pointing to the left and with increasing anodic currents pointing downwards. Cyclic voltammetry (CV) was conducted with the use of a three-electrode cell in which ITO (polymer films area about 0.5 cm × 1.1 cm) was used as a working electrode. A platinum wire was used as an auxiliary electrode. All cell potentials were taken by using a homemade Ag/AgCl, KCl (sat.) reference electrode. Spectroelectrochemical experiments were carried out in a cell built from a 1 cm commercial UV–vis cuvette using Hewlett–Packard 8453 UV–vis diode array spectrophotometer. The ITO-coated glass slide was used as the working electrode, a platinum wire as the counter electrode, and a Ag/AgCl cell as the reference electrode. CE (η) determines the amount of optical density change (δOD) at a specific absorption wavelength induced as a function of the ejected/injected charge (Q_r; also termed as electroactivity) which is determined from the *in situ* experiments. CE is given by the equation: $\eta = \delta OD/Q = \log[T_b/T_c]/Q$, where η (cm^2/C) is the coloration efficiency at a given wavelength, Q is the injected charge, and T_b and T_c are the bleached and colored transmittance values, respectively. The thickness of the polyamide thin films was measured by alpha-step profilometer (Kosaka Lab., Surfcorder ET3000, Japan).

3. Results and discussion

3.1. Polymer synthesis

Two series of polyamides **I-II** containing aniline- and DPA-derivatives units were prepared from diamines **1** and **2** with two commercially available diacid chlorides **3a** and **3b**, respectively (Scheme 1). The polycondensation was carried out *via* low-temperature solution method using propylene oxide or calcium oxide as an acid acceptor. All the polymerization proceeded homogeneously and gave high molecular weights. The obtained polyamides had inherent viscosities in the range of 0.51–0.80 dL/g with weight-average molecular weights (M_w) and polydispersity (PDI) of 83,000–102,000 daltons and 1.42–1.54, respectively, relative to polystyrene standards (Table S1). All the polymers could afford tough and free-standing films *via* solution casting. The formation of polyamides was confirmed with FT-IR and NMR spectroscopy (as shown in Figs. S1 and S2). The FT-IR spectra of polyamide **IIb** exhibited characteristic absorption bands of the amide group at around 3330 cm^{-1} (N-H stretch) and 1651 cm^{-1} (amide carbonyl). The structural compositions of these polyamides were also verified by the high resolution NMR spectra. A structurally related polyamide **IIIb** derived from diamine

Table 1
Thermal properties of polyamides.

Polymer[a]	T_g (°C)[b]	T_d^5 (°C)[c]		T_d^{10} (°C)[c]		R_{w800} (%)[d]
		N_2	Air	N_2	Air	
Ia	270	400	420	435	440	55
Ib	275	415	400	495	430	58
IIa	252	540	525	585	575	76
IIb	255	540	500	575	560	72

[a] The polymer film samples were heated at 300 °C for 1 h prior to all the thermal analyses.
[b] Midpoint temperature of baseline shift on second DSC heating trace (rate 20 °C/min) of the sample after quenching from 400 °C.
[c] Temperature at which 5% and 10% weight loss occurred, respectively, by TGA at a heating rate of 20 °C/min and a gas flow rate of 20 cm^3/min.
[d] Residual weight percentages at 800 °C under nitrogen flow.

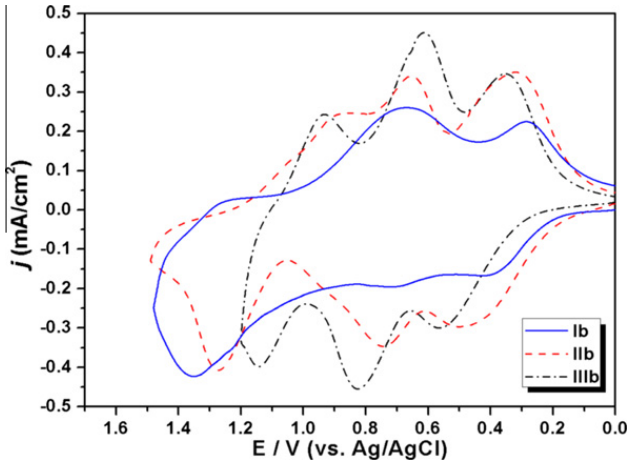

Fig. 1. Cyclic voltammograms of polyamide **Ib**, **IIb**, and **IIIb** films on an ITO-coated glass substrate in CH_3CN containing 0.1 M TBAP. Scan rate = 50 mV/s.

3 was used for comparison studies. The synthesis of polymer **IIIb** has been described previously [8l].

3.2. Basic characterization

The solubility properties of polyamides **I**-**II** in some organic solvents were investigated, and the results are listed in Table S2 in Supporting information. Due to the strong hydrogen bonding interaction and less steric hindrance for close packing, the polymer **I** series exhibited lower solubility among these polyamides. While polyamides **II** with packing-disruptive TPA-derivatives showed the better solubility, and make these polymers as potential candidates for practical applications by spin-coating or inkjet-printing processes to afford high performance thin films for optoelectronic devices. The thermal properties of these polyamides measured by TGA and DSC are summarized in Table 1. Typical TGA curves of polyamides **Ib** and **IIb** in both air and nitrogen atmospheres are depicted in Fig. S3. All the prepared polyamides exhibited good thermal stability with insignificant weight loss up to 350 °C under nitrogen or air atmosphere. The 10% weight-loss temperature of these polymers in nitrogen and air were recorded in the range of 435–585 and 430–575 °C, respec-

Table 2
Redox potentials and energy levels of polyamides.

Code	Thin films	Oxidation[a]				E_g/eV[b]	HOMO[c]	LUMO
	λ_{onset}	E_{onset}	$E_{1/2(ox1)}$	$E_{1/2(ox2)}$	$E_{1/2(ox3)}$			
Ia	657	0.18	0.34	0.67	1.41[d]	1.89	4.70	2.81
Ib	682	0.20	0.35	0.69	1.35[d]	1.82	4.71	2.89
IIa	446	0.23	0.37	0.66	1.23[d]	2.78	4.73	1.95
IIb	454	0.24	0.41	0.70	1.27[d]	2.73	4.77	2.04
IIIb	443	0.27	0.45	0.71	1.04	2.80	4.81	2.01

[a] Versus Ag/AgCl in CH_3CN. $E_{1/2}$: average potential of the redox couple peaks.
[b] Bandgaps calculated from absorption edge of the polymer films: $E_g = 1240/\lambda_{onset}$.
[c] The HOMO energy levels were calculated from cyclic voltammetry and were referenced to ferrocene (4.8 eV; $E_{1/2}$ = 0.44 V).
[d] Irreversible peak potential.

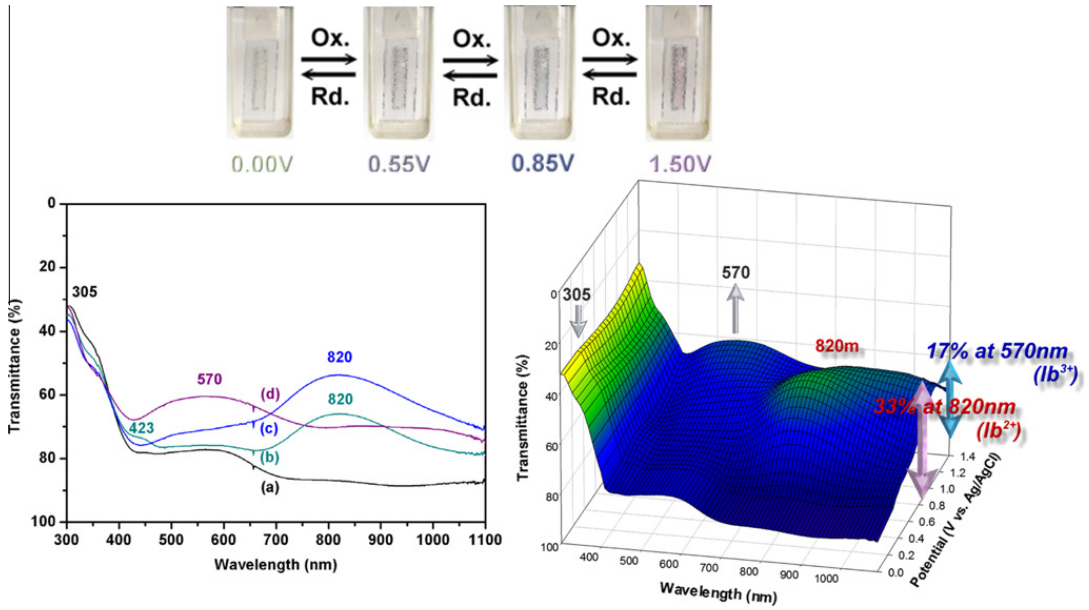

Fig. 2. Electrochromic behavior (left) at applied potentials of (A) 0.00, (B) 0.55, (C) 0.85, (D) 1.50 (V versus Ag/AgCl), and 3D spectroelectrochemical behavior (right) from 0.00 to 1.50 (V versus Ag/AgCl) of polyamide **Ib** thin film (~270 nm in thickness) on the ITO-coated glass substrate (coated area: 1.1 cm × 0.3 cm) in 0.1 M TBAP/CH_3CN.

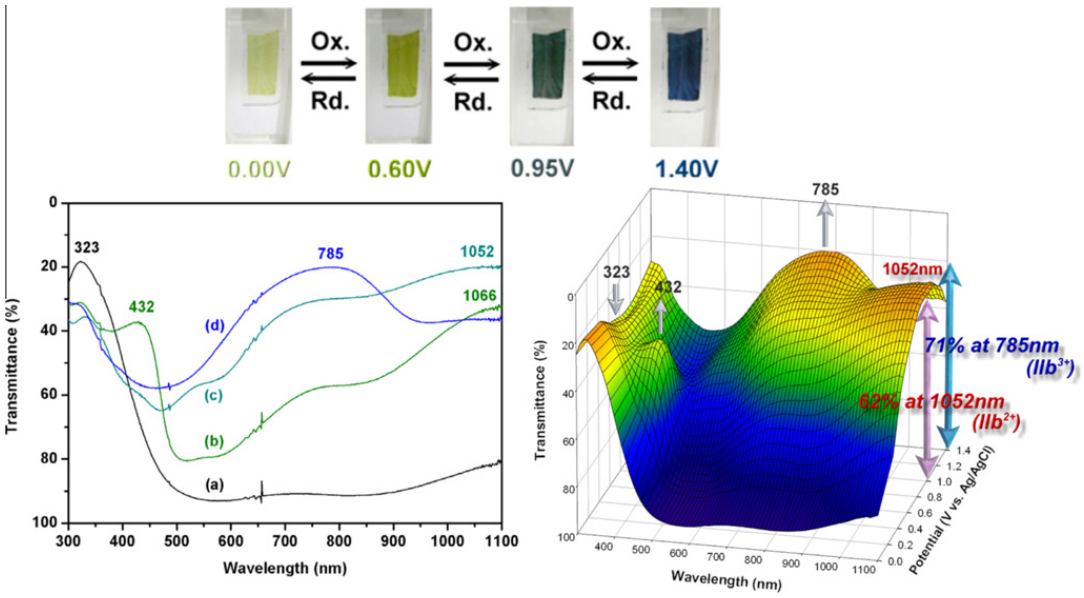

Fig. 3. Electrochromic behavior (left) at applied potentials of (A) 0.00, (B) 0.60, (C) 0.95, (D) 1.40 (V versus Ag/AgCl), and 3D spectroelectrochemical behavior (right) from 0.00 to 1.40 (V versus Ag/AgCl) of polyamide **IIb** thin film (~260 nm in thickness) on the ITO-coated glass substrate (coated area: 1.0 cm × 0.5 cm) in 0.1 M TBAP/CH_3CN.

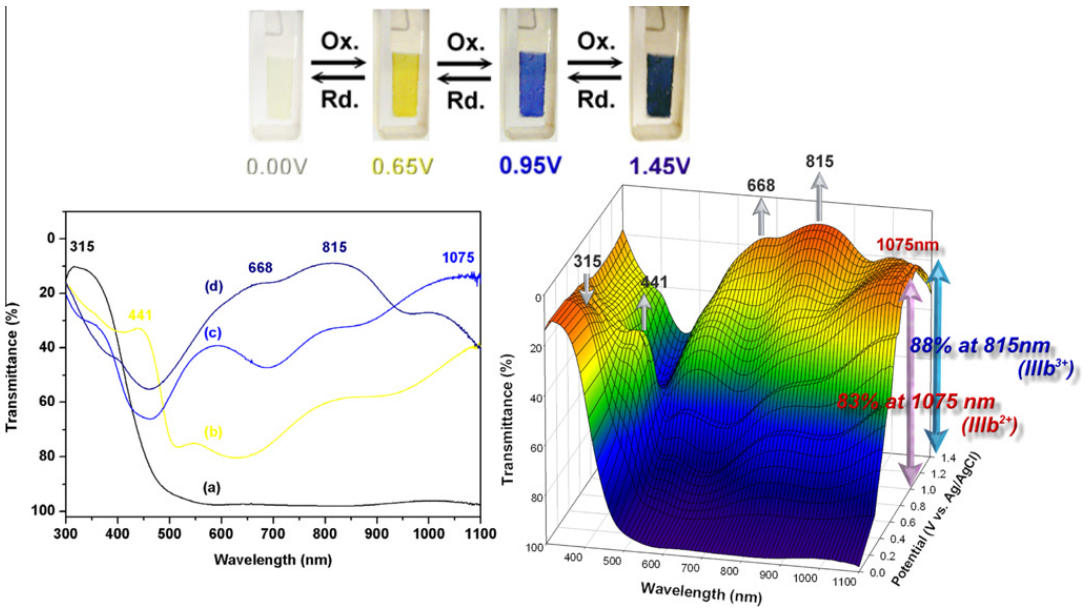

Fig. 4. Electrochromic behavior (left) at applied potentials of (A) 0.00, (B) 0.65, (C) 0.95, (D) 1.45 (V versus Ag/AgCl), and 3D spectroelectrochemical behavior (right) from 0.00 to 1.45 (V versus Ag/AgCl) of polyamide **IIIb** thin film (~260 nm in thickness) on the ITO-coated glass substrate (coated area: 1.1 cm × 0.5 cm) in 0.1 M TBAP/CH_3CN.

tively. The amount of carbonized residue (char yield) of these polymers in nitrogen atmosphere was more than 55% at 800 °C. The high char yields of these polymers can be ascribed to their high aromatic content. The lowest T_d value of polyamide **I** series could be explained in terms of the less aromatic segment in its backbone. The glass-transition temperature (T_g) of these polyamides in the range of 252–275 °C summarized in the Table 1 could be easily observed by the DSC measurements (as shown in Fig. S4 of the Supporting information), and polyamide **I** series revealed a higher T_g that could be attributed to the strong interaction of hydrogen bonding between the secondary amino and carbonyl groups in the polymer chains.

3.3. Electrochemical properties

The electrochemical behavior of the polyamides was investigated by cyclic voltammetry (CV) conducted for the cast film on an indium-tin oxide (ITO)-coated glass slide as working electrode in anhydrous acetonitrile (CH_3CN) using 0.1 M of tetrabutylammonium perchlorate (TBAP) as a supporting electrolyte under nitrogen

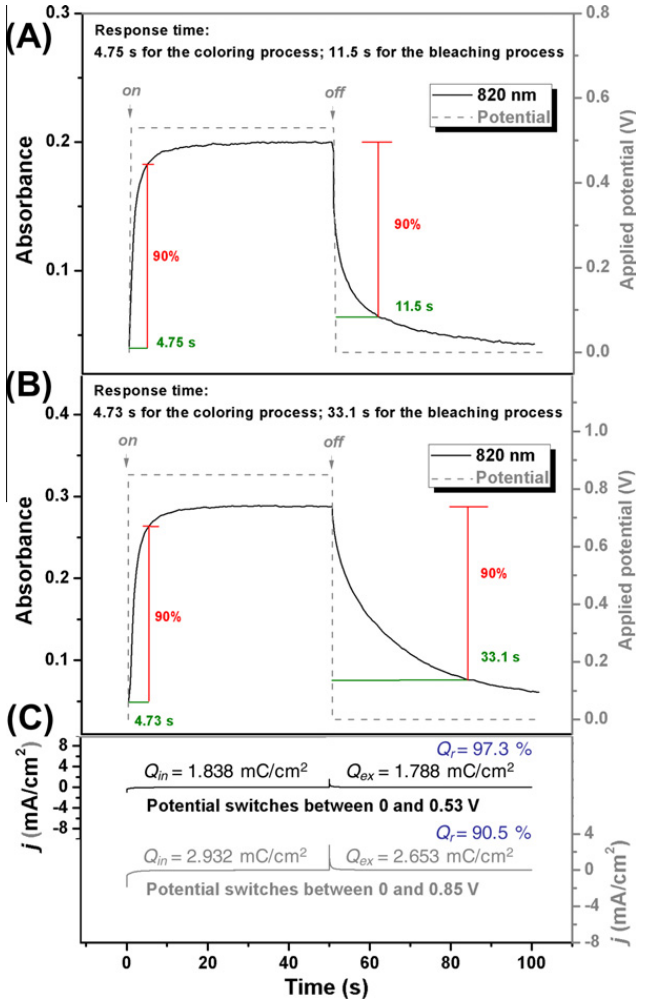

Fig. 5. Calculation of optical response time (A) 820 nm at the applied potential of 0.53 V (B) 820 nm at the applied potential of 0.85 V (C) current–time curves of polyamide **Ib** thin film (~270 nm in thickness) coated on the ITO-coated glass substrate (coated area: 1.1 cm × 0.5 cm) in 0.1 M TBAP/CH_3CN.

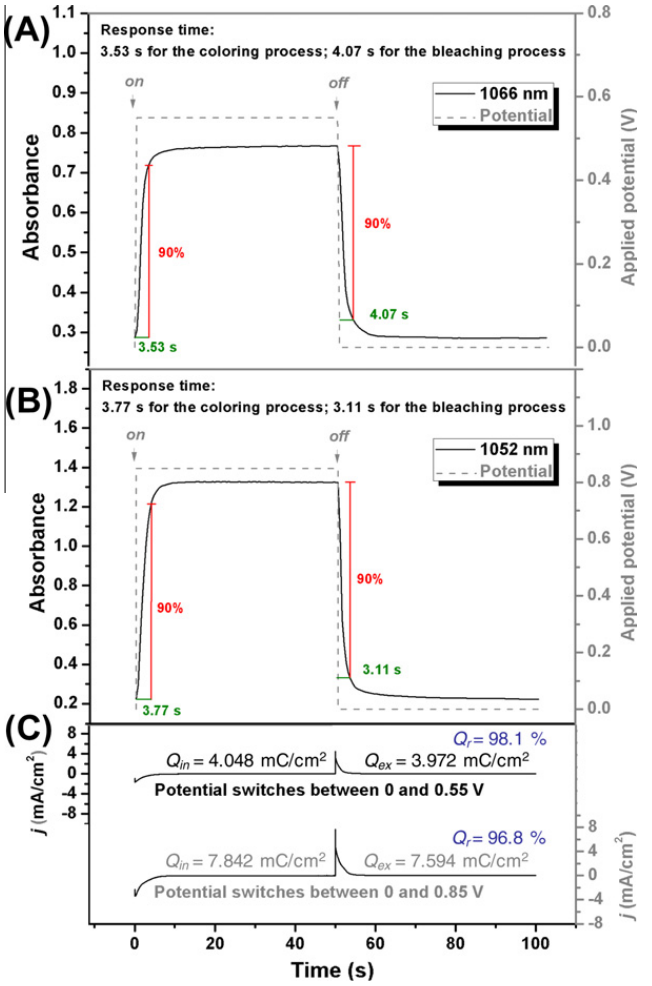

Fig. 6. Calculation of optical response time (A) 1066 nm at the applied potential of 0.55 V (B) 1052 nm at the applied potential of 0.85 V (C) current–time curves of polyamide **IIb** thin film (~260 nm in thickness) coated on the ITO-coated glass substrate (coated area: 1.1 cm × 0.5 cm) in 0.1 M TBAP/CH_3CN.

atmosphere. The typical CV diagrams of polyamides **Ib**, **IIb**, and **IIIb** are shown in Fig. 1 for comparison. All the polyamides exhibited two reversible oxidation redox couples and one irreversible redox peak, while polyamide **IIIb** revealed three reversible oxidation redox steps with the highest E_{onset} of 0.27 V as compared with others. Thus, the incorporation of 4-methoxy-substituted phenyl groups into the electroactive nitrogen site of amino moieties to replace hydrogen atom increased the applied potential values of the first oxidation stage, but these extra phenyl rings with electron-donating methoxy groups could provide the additional resonance routes to stabilize the cation radical formed during oxidation procedure, and therefore revealing higher reversibility in CV measurements. The redox potentials of the polyamides as well as their respective highest occupied molecular orbital (HOMO) and lowest unoccupied molecular orbital (LUMO) (versus vacuum) are calculated and summarized in Table 2. The HOMO level or called ionization potentials (versus vacuum) of polyamides are estimated from the $E_{1/2}$ value of their oxidation in CV experiments as 4.70–4.81 eV (on the basis that ferrocene/ferrocenium is 4.8 eV below the vacuum level with $E_{1/2}$ = 0.44 V).

3.4. Spectroelectrochemistry

Spectroelectrochemical experiments were used to evaluate the optical properties of these electrochromic materials. For the investigations, the polyamide films were cast on an ITO-coated glass slide, and a homemade electrochemical cell was built from a commercial ultraviolet (UV)-visible cuvette. The cell was placed in the optical path of the sample light beam in a UV–vis spectrophotometer, which allowed us to acquire electronic absorption spectra under potential control in a 0.1 M TBAP/CH_3CN solution. The typical spectroelectrochemistry and three-dimentional % transmittance-wavelength-applied potential correlation of polyamide **Ib**, **IIb**, and **IIIb** films are presented in Figs. 2–4, respectively. The **Ib** film exhibited strong absorption at around 305 nm, characteristic for aromatic phenyl ring in the neutral form (0.00 V) with a color of pale green in the visible region. Upon oxidation (increasing applied

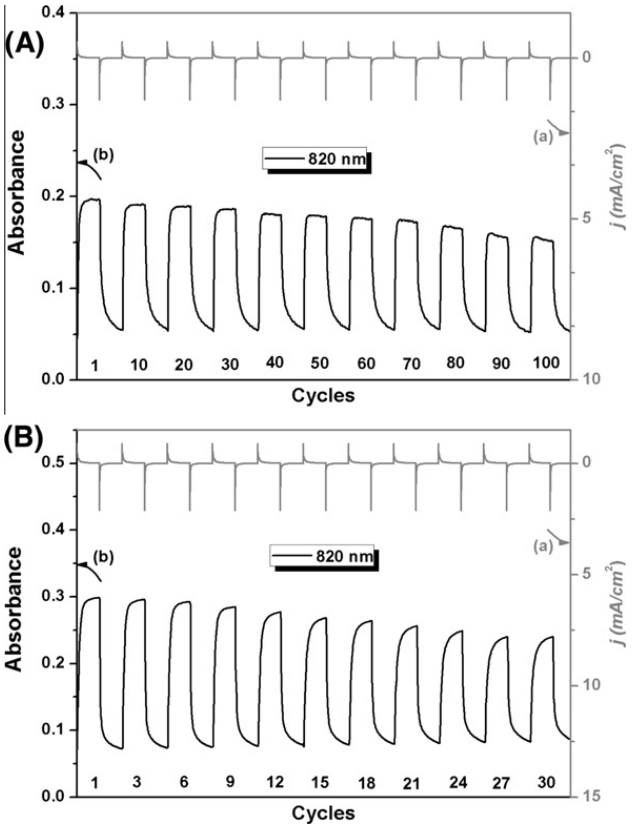

Fig. 7. Electrochromic switching between (A) 0 and 0.53 V and (B) 0 and 0.85 V (versus Ag/AgCl) of polyamide **Ib** thin film (~270 nm in thickness) on the ITO-coated glass substrate (coated area: 1.1 cm × 0.5 cm) in 0.1 M TBAP/CH_3CN with a cycle time of 60 s. (a) Current consumption and (b) absorbance change monitored at the given wavelength.

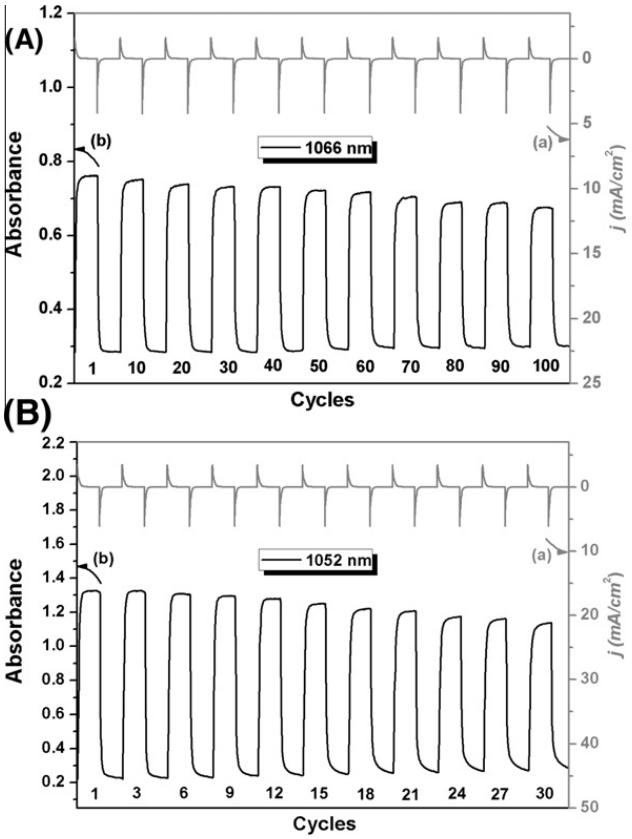

Fig. 8. Electrochromic switching between (A) 0 and 0.55 V and (B) 0 and 0.85 V (versus Ag/AgCl) of polyamide **IIb** thin film (~260 nm in thickness) on the ITO-coated glass substrate (coated area: 1.1 cm × 0.5 cm) in 0.1 M TBAP/CH_3CN with a cycle time of 60 s. (a) Current consumption and (b) absorbance change monitored at the given wavelength.

voltage from 0.00 to 0.55 V), the intensity of the absorption peak at 305 nm gradually decreased while a new peak at 423 nm and an intervalence charge transfer (IV-CT) absorption band centered around 820 nm in the NIR region gradually increased due to the formation of a monocation radical of the diphenylamine moiety [9]. Furthermore, the broad absorption in NIR region could be attributed the result of IV-CT excitation between states in which the positive charge is centered at different nitrogen atoms, and that is consistent with the phenomenon classified by Robin and Day [10]. As the higher anodic potential to 0.85 V corresponding to $\mathbf{Ib}^{2+}$, the absorption bands (305, and 423 nm) decreased gradually while a broad band between 700 and 950 nm increased continuously. By further applying positive potential value up to 1.50 V corresponding to $\mathbf{Ib}^{3+}$, the characteristic absorbance at 570 nm increased slightly. From the spectra shown in Fig. 2, the polyamide **Ib** film revealed low color contrast and optical transmittance change ($\Delta T\%$) of 33% at 820 nm for light blue in second oxidation stage, and only 17% at 570 nm for the light purple in third oxidation stage, respectively. While the **IIb** film exhibited strong characteristic absorption of triphenylamine at around 323 nm in the neutral form (0 V) with very pale greenish color, which is shown in the Fig. 3. Upon oxidation (increasing applied voltage from 0 to 0.60 V), the intensity of the absorption peak at 323 nm gradually decreased while a new peak at 432 nm and a broad IV-CT band centered around 1066 nm in the NIR region gradually increased in intensity. We attribute the spectral change in visible-light range to the formation of a stable monocation radical $\mathbf{IIb}^{1+}$ at the central TPA moiety. As increasing potential to 0.95 V corresponding to $\mathbf{IIb}^{2+}$, the absorption bands (323 and 432 nm) decreased gradually with new broad band centered at around 1052 nm in the NIR region. When the applied potential was added to 1.40 V, the absorption bands at 1052 nm decreased gradually with a new broad band centered at around 785 nm. The disappearance of NIR absorption band can be ascribed to the further oxidation of $\mathbf{IIb}^{2+}$ species to the formation of $\mathbf{IIb}^{3+}$ in the diphenylamine segments. Meanwhile, the color of the film changed from pale greenish neutral state to the lawn-green/green semi-oxidation states, and deep blue fully oxidation state. From the inset shown in Fig. 3, the polymer **IIb** exhibited highly optical transmittance change ($\Delta T\%$) of 62% at 1052 nm for green coloring at the second oxidation stage, and 71% at 785 nm for deep blue coloring at third oxidation stage, respectively. The similar experiment results of the **IIIb** film was depicted in Fig. 4. The polyamide **IIIb** film could switch from original colorless to yellow/blue, and then to a deep blue oxidation state.

From the inset shown in Fig. 4, the TPA-based polyamide **IIIb** revealed even higher optical transmittance change ($\Delta T\%$) up to 83% at 1075 nm for blue (second oxidation

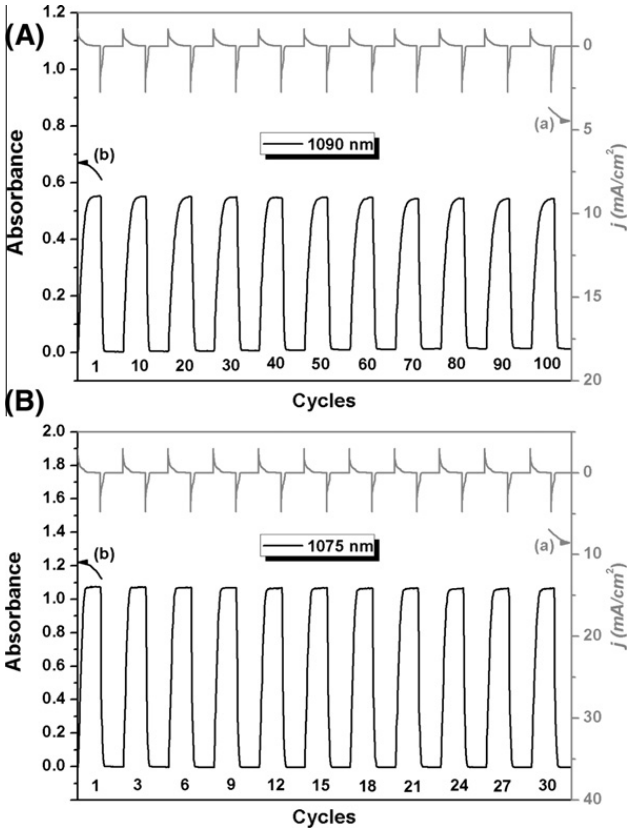

Fig. 9. Electrochromic switching between (A) 0 and 0.62 V and (B) 0 and 0.90 V (versus Ag/AgCl) of polyamide **IIIb** thin film (~260 nm in thickness) on the ITO-coated glass substrate (coated area: 1.1 cm × 0.5 cm) in 0.1 M TBAP/CH_3CN with a cycle time of 60 s. (a) Current consumption and (b) absorbance change monitored at the given wavelength.

stage), and 88% at 815 nm for deep blue (third oxidation stage), respectively. Comparing the optical transmittance changes of these three type series, the TPA-based polyamides exhibited higher contrast than DPA-based polyamides. The film colorations could be distributed homogeneously across polymer film and survived for more than hundred redox cycles.

3.5. Electrochromic switching studies

For electrochromic switching studies, the polymer films were cast on ITO-coated glass slides in the same manner as described above, then chronoamperometric and absorbance measurements were performed. When the films were electrically switched, the absorbance at the given wavelength was monitored as a function of time by UV–vis spectroscopy. Switching results for the representative cast film of polyamides **Ib** and **IIb** are summarized in Figs. 5 and 6 for comparison. The switching time was calculated at 90% of the full switch because it is difficult to perceive any further color change with naked eye beyond this point. Comparing the response time of these two series, the polyamide **IIb** (Fig. 6) showed faster response time than **Ib** (Fig. 5). When the potential was switched between 0.00 and 0.55 V for the polyamide **IIb**, the time for coloring and bleaching were 3.53 and 4.07 s, respectively, with 98% of the ratio of the charge density. While the switching potential was set between 0.00 and 0.90 V, the polyamide **IIb** thin film required 3.77 s for coloration and 3.11 s for bleaching with 97% of the ratio of the charge density. It is noteworthy that the coloring of DPA-based polyamide **Ib** proceeded during the anodic oxidation faster than the bleaching in the reverse cathodic reduction process, which is very similar to polyaniline system. This phenomenon was also described and discussed in the previous reports [9,11]. The ratio of extracted/injected charge (Q_r) was calculated by integration of the current density and time obtained from Figs. 5(c) and 6(c) for oxidation and reduction process at the first and second oxidation stage, respectively. The electrochromic stability of these polyamide **Ib**, **IIb** and **IIIb** films were also determined by measuring the optical change as a function of the number of switching cycles (Figs. 7–9). The coloration efficiency, CE ($\eta = \delta OD/Q$), and injected charge (Q) at different switching steps were summarized in Tables 3 and 4. After continuous 100 cyclic scanning at the first oxidation stage, the polyamide **Ib** film reduced electroactivity obviously [Fig. 7(A)]. On the contrary, the polymer **IIIb** exhibited high CE up to 167 cm^2/C at 1090 nm, and showed highly stable electrochromic

Table 3
Optical and electrochemical data collected for coloration efficiency measurements of polyamide **Ib**-**IIIb**.

Cycling times[a]	δOD_{820}[b] **Ib**	δOD_{1066}[b] **IIb**	δOD_{1090}[b] **IIIb**	Q (mC/cm^2)[c]			η (cm^2/C)[d]			Decay (%)[e]		
				Ib	**IIb**	**IIIb**	**Ib**	**IIb**	**IIIb**	**Ib**	**IIb**	**IIIb**
1	0.152	0.476	0.551	1.838	4.048	3.302	83	118	167	0	0	0
10	0.148	0.469	0.551	1.838	4.048	3.302	81	116	167	2.41	1.69	0
20	0.147	0.463	0.551	1.837	4.047	3.302	80	114	167	3.61	3.39	0
30	0.144	0.460	0.551	1.837	4.047	3.302	78	114	167	6.02	3.39	0
40	0.139	0.460	0.551	1.837	4.047	3.302	76	114	167	8.43	3.39	0
50	0.137	0.456	0.551	1.835	4.047	3.302	75	113	167	9.64	4.24	0
60	0.133	0.451	0.551	1.836	4.046	3.302	72	111	167	13.3	5.93	0
70	0.127	0.440	0.551	1.834	4.044	3.302	69	109	167	16.9	7.63	0
80	0.115	0.424	0.551	1.835	4.045	3.302	63	105	167	24.1	12.4	0
90	0.103	0.424	0.551	1.832	4.043	3.302	56	105	167	32.5	12.4	0
100	0.098	0.418	0.551	1.829	4.043	3.302	54	103	167	34.9	12.7	0

[a] Switching between 0 and 0.53 for **Ib**, 0 and 0.55 for **IIb**, and 0 and 0.62 for **IIIb** (V versus Ag/AgCl).
[b] Optical density change at the given wavelength.
[c] Ejected charge, determined from the *in situ* experiments.
[d] Coloration efficiency is derived from the equation $\eta = \delta OD/Q$.
[e] Decay of coloration efficiency after cyclic scans.

Table 4
Optical and electrochemical data collected for coloration efficiency measurements of polyamide **Ib-IIIb.**

Cycling times[a]	δOD_{820}[b] **Ib**	δOD_{1052}[b] **IIb**	δOD_{1075}[b] **IIIb**	Q (mC/cm^2)[c]			η (cm^2/C)[d]			Decay (%)[e]		
				Ib	**IIb**	**IIIb**	**Ib**	**IIb**	**IIIb**	**Ib**	**IIb**	**IIIb**
1	0.227	1.100	1.070	2.932	7.842	5.466	77	140	196	0	0	0
3	0.224	1.100	1.070	2.932	7.842	5.466	76	140	196	1.30	0	0
6	0.218	1.069	1.070	2.932	7.842	5.466	74	136	196	3.90	2.86	0
9	0.209	1.051	1.070	2.931	7.840	5.466	71	134	196	7.79	4.29	0
12	0.205	1.042	1.070	2.930	7.840	5.466	70	133	196	9.09	5.00	0
15	0.197	1.002	1.070	2.930	7.838	5.466	67	128	196	13.0	8.57	0
18	0.189	0.969	1.070	2.930	7.838	5.466	65	124	196	15.6	11.4	0
21	0.178	0.956	1.070	2.929	7.838	5.466	61	122	196	20.8	12.9	0
24	0.166	0.921	1.070	2.930	7.837	5.466	57	118	196	26.0	15.7	0
27	0.160	0.903	1.070	2.926	7.836	5.466	55	115	196	28.6	17.9	0
30	0.157	0.877	1.070	2.926	7.833	5.466	54	112	196	29.9	20.0	0

[a] Switching between 0 and 0.85 for **Ib**, 0 and 0.85 for **IIb**, and 0 and 0.90 for **IIIb** (V versus Ag/AgCl).
[b] Optical density change at the given wavelength.
[c] Ejected charge, determined from the *in situ* experiments.
[d] Coloration efficiency is derived from the equation $\eta = \delta OD/Q$.
[e] Decay of coloration efficiency after cyclic scans.

behavior without any decay [Fig. 9(A)]. As the applied switching potential increased to the second oxidation stage, the polymer **IIIb** still exhibited excellent stability of electrochromic characteristics and high CE (196 cm^2/C at 1075 nm) after 30 cycles [Fig. 9(B)]. These results were also consistent with the above-mentioned assumption that the incorporating 4-methoxyphenyl moieties into the electroactive nitrogen atom of amino groups could effectively stabilize the cation radicals by the additional extra resonance routes.

Furthermore, we also fabricated single layer electrochromic cells as preliminary investigation (Fig. 10). The polyamide films were coated onto ITO-glass and then dried. Then, the gel electrolyte was spread on the polymer coated side of the electrode and the electrodes were sandwiched. To prevent leakage, an epoxy resin was applied to seal the device. As a typical example, an electrochromic cell based on polyamide **IIb** was fabricated, and the polymer film was pale green at neutral form. When the voltage was applied (from 0.0 to 1.0 V, 2.0 V and 3.0 V, respectively), the color changed tolawn-green, green, and deep blue, respectively, the same as those were already observed in the spectroelectrochemical experiments. When the potential was subsequently set back at 0.0 V, the polymer film turned back to original color. We believe that optimization could further improve the device performance and fully explore the potential of these electrochromic polyamides.

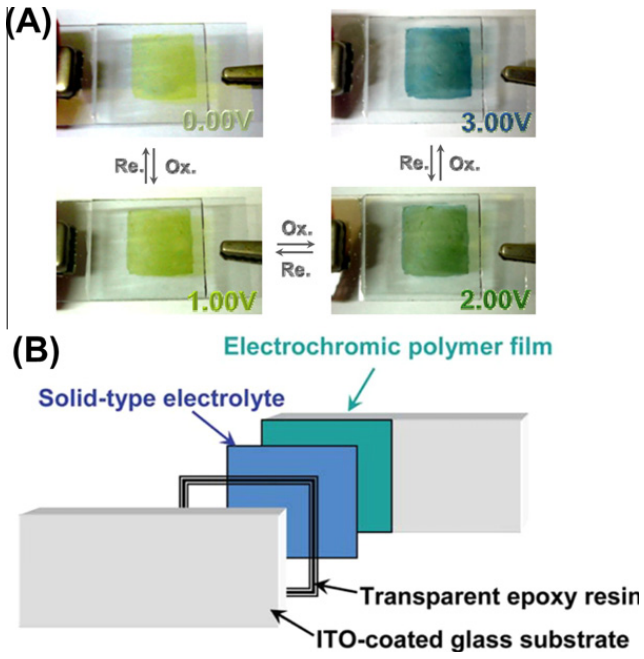

Fig. 10. (A) Photographs of single-layer ITO-coated glass electrochromic device, using polyamide **IIb** as active layer. (B) Schematic diagram of polyamide electrochromic device sandwichcell.

4. Conclusions

Two series of novel NIR electrochromic aromatic polyamides containing electroactive DPA or TPA moieties were prepared from the diamine monomers, 4,4′-bis[(4-aminophenyl)amino]-diphenylamine (**1**), and 4,4′-bis[(4-aminophenyl)amino]-4″-methoxytriphenylamine (**2**), with diacid chlorides *via* the low-temperature polycondensation. The introduction of 4-methoxy-substituted phenyl groups into the nitrogen atom position not only improved the solubility but also enhanced thermal stability of the resultant polyamides. In addition, there are two basic conclusions; series of new ambipolar polyamides containing amine-derivatives with different degree of 4-methoxyphenyl substituent showing anodically/cathodically electrochromic characteristic, and the results demonstrated that the non-conjugated TPA-based polyamides revealed more stable electrochemical oxidation behavior and better coloring contrast and electrochromic reversibility than conjugated DPA-based corresponding polyamides due to the additional phenyl ring providing the route to stabilize the cation radical formed during oxidation.

Acknowledgement

The authors are grateful to the National Science Council of the Republic of China for its financial support of this work.

Appendix A. Supplementary data

Supplementary data associated with this article can be found, in the online version, at doi:10.1016/j.orgel.2012.01.025.

References

[1] T. Kobayashi, H. Yoncyama, H. Amura, J. Electroanal. Chem. Interf. Electrochem. 161 (1984) 419–423.

[2] (a) K. Kaneto, M. Kaneko, Y. Min, A.G. MacDiarmid, Synth. Met. 71 (1995) 2211–2212;
(b) W. Takashima, M. Haneko, K. Kaneto, A.G. MacDiarmid, Synth. Met. 71 (1995) 2265–2266;
(c) J.M. Sansiñena, J. Gao, H.L. Wang, Adv. Funct. Mater. 13 (2003) 703–709;
(d) J. Gao, J.M. Sansiñena, H.L. Wang, Chem. Mater. 15 (2003) 2411–2418.

[3] A.G. MacDiarmid, S.L. Mu, N.L.D. Somasiri, W. Wu, Mol. Cryst. Liq. Cryst. 121 (1985) 187–190.

[4] (a) D.W. Deberry, J. Electrochem. Soc. 132 (1985) 1022–1026;
(b) N. Ahmad, A.G. MacDiarmid, Synth. Met. 78 (1996) 103–110;
(c) W.K. Lu, R.L. Elsenbaumer, B. Wessling, Synth. Met. 71 (1995) 2163–2166.

[5] (a) D. Chao, X. Lu, J. Chen, X. Liu, W. Zhang, Y. Wei, Polymer 47 (2006) 2643–2648;
(b) J. Zhang, D. Chao, L. Cui, X. Liu, W. Zhang, Macromol. Chem. Phys. 210 (2009) 1739–1745;
(c) L. Cui, D. Chao, J. Zhang, H. Mao, Y. Li, C. Wang, Synth. Met. 160 (2010) 400–404.

[6] J. Gao, D.G. Liu, J.M. Sansiñena, H.L. Wang, Adv. Funct. Mater. 14 (2004) 537–543.

[7] (a) Y. Imai, High Perform. Polym. 7 (1995) 337–345; (b) Y. Imai, React. Funct. Polym. 30 (1996) 3–15; (c) G.S. Liou, J. Polym. Sci. Part A: Polym. Chem. 36 (1998) 1937–1943; (d) G.C. Eastmond, J. Paprotny, R.S. Irwin, Polymer 40 (1999) 469–486; (e) G.C. Eastmond, M. Gibas, J. Paprotny, Eur. Polym. J. 35 (1999) 2097–2106; (f) D.S. Reddy, C.H. Chou, C.F. Shu, G.H. Lee, Polymer 44 (2003) 557–563; (g) W.M. Li, S.H. Li, Q.Y. Zhang, S.B. Zhang, Macromolecules 40 (2007) 8205–8211.

[8] (a) S.H. Cheng, S.H. Hsiao, T.H. Su, G.S. Liou, Macromolecules 38 (2005) 307–316; (b) T.H. Su, S.H. Hsiao, G.S. Liou, J. Polym. Sci. Part A: Polym. Chem. 43 (2005) 2085–2098; (c) C.W. Chang, G.S. Liou, S.H. Hsiao, J. Mater. Chem. 17 (2007) 1007–1015; (d) G.S. Liou, C.W. Chang, Macromolecules 41 (2008) 1667–1674; (e) S.H. Hsiao, G.S. Liou, Y.C. Kung, H.J. Yen, Macromolecules 41 (2008) 2800–2808; (f) C.W. Chang, C.H. Chung, G.S. Liou, Macromolecules 41 (2008) 8441–8451; (g) C.W. Chang, G.S. Liou, J. Mater. Chem. 18 (2008) 5638–5646; (h) C.W. Chang, H.J. Yen, K.Y. Huang, J.M. Yeh, G.S. Liou, J. Polym. Sci. Part A: Polym. Chem. 46 (2008) 7937–7949; (i) H.J. Yen, G.S. Liou, Chem. Mater. 21 (2009) 4062–4070; (j) S.H. Hsiao, G.S. Liou, H.M. Wang, J. Polym. Sci. Part A: Polym. Chem. 47 (2009) 2330–2343; (k) G.S. Liou, H.Y. Lin, H.J. Yen, J. Mater. Chem. 19 (2009) 7666–7673; (l) G.S. Liou, H.Y. Lin, Macromolecules 42 (2009) 125–134; (m) L.T. Huang, H.J. Yen, C.W. Chang, G.S. Liou, J. Polym. Sci. Part A: Polym. Chem. 48 (2010) 4747–4757; (n) H.J. Yen, S.M. Guo, G.S. Liou, J. Polym. Sci. Part A: Polym. Chem. 48 (2010) 5271–5281; (o) H.J. Yen, G.S. Liou, J. Mater. Chem. 20 (2010) 9886–9894; (p) H.J. Yen, H.Y. Lin, G.S. Liou, Chem. Mater. 23 (2011) 1874–1882; (q) H.J. Yen, S.M. Guo, J.M. Yeh, G.S. Liou, J. Polym. Sci. Part A: Polym. Chem. 49 (2011) 3637–3646; (r) H.J. Yen, S.M. Guo, G.S. Liou, J.C. Chung, Y.C. Liu, Y.F. Lu, Y.Z. Zeng, J. Polym. Sci. Part A: Polym. Chem. 49 (2011) 3805–3816; (s) H.J. Yen, K.Y. Lin, G.S. Liou, J. Polym. Sci. Part A: Polym. Chem. 50 (2012) 61–69. (t) H.J. Yen, G.S. Liou, Polym. Chem. 3 (2012) 255–264.

[9] L.T. Huang, H.J. Yen, G.S. Liou, Macromolecules 44 (2011) 9595–9610.

[10] (a) C. Creutz, H. Taube, J. Am. Chem. Soc. 95 (1973) 1086–1094;
(b) C. Lambert, G. Noll, J. Am. Chem. Soc. 121 (1999) 8434–8442.

[11] A. Malinauskas, R. Holze, Synth. Met. 97 (1998) 31–36.